Rare Metal Materials and Engineering
Volume 50, Issue 9, September 2021
Available online at www.rmme.ac.cn

Science Press

Cite this article as: Zhang Wenlong, Wang Ying, Wang Dongzheng, et al. Modification and Influence of Screen-Printed Graphene Oxide on $LiNi_{1/3}Co_{1/3}Mn_{1/3}O_2$ Ternary Cathode and Properties of Lithium Ion Battery [J]. Rare Metal Materials and Engineering, 2021, 50(09): 3144-3148.

ARTICLE

Modification and Influence of Screen-Printed Graphene Oxide on $LiNi_{1/3}Co_{1/3}Mn_{1/3}O_2$ Ternary Cathode and Properties of Lithium Ion Battery

Zhang Wenlong[1], Wang Ying[1,2], Wang Dongzheng[1], Lu Chunchi[1], Yan Xiao[1], Huang Bixiong[1]

[1] School of Mechanical and Automotive Engineering, Shanghai University of Engineering Science, Shanghai 201620, China; [2] Jiangsu Laboratory of Lake Environment Remote Sensing Technologies, Huaiyin Institute of Technology, Huaian 223003, China

Abstract: Electrodes consisting of $LiNi_{1/3}Co_{1/3}Mn_{1/3}O_2$, aluminum foil, conductive additives, and polyvinylidene fluoride were coated with a thin graphene oxide layer via a simple screen-printing method. The cycle performance and rate capability were tested at a cut-off voltage of 4.3 V. Results show that the capacity deceases whereas the polarization increases during the galvanostatic charge-discharge tests for primary electrodes. For the graphene-oxide-modified electrodes, the capacity decrement reduces and polarization increment rate evidently slows down. As a result, the cycle stability and rate capability are improved because the graphene oxide coating suppresses the side reactions between the $LiNi_{1/3}Co_{1/3}Mn_{1/3}O_2$ electrodes and electrolyte. The research provides an ecofriendly and highly effective strategy to improve the performance of $LiNi_{1/3}Co_{1/3}Mn_{1/3}O_2$ electrodes.

Key words: $LiNi_{1/3}Co_{1/3}Mn_{1/3}O_2$; cathode; graphene oxide; screen-printing; lithium ion battery

Layered lithium metal oxides $LiMO_2$ (M=Ni, Co, Mn, Al) are considered as the most promising cathodes due to their high energy density[1-3]. Among the oxides, $LiNi_xMn_xCo_{1-2x}O_2$ ($x\leqslant0.5$) shows high capacity, excellent thermal stability, low cost, and high safety[4,5]. Significant improvement has been achieved for the rate capability and cycle performance[6-10]. However, the instability is still a key problem. Many researches reveal that the thickening of solid electrolyte interphase (SEI) film caused by the transition metals escaping from the active material is an unstable factor[11-15].

Surface coating is widely used to retard the dissolution of transition metals into the interface of the active material and electrolyte[7,16-18], thereby improving the stability of SEI film process. In recent researches, the transition metal oxide particles are coated with thin films, which are usually poor conductors of electronics or lithium ions. Another way to stabilize SEI film is to deposit a thin film on the finished electrodes. This method has been employed to modify cathode and anode electrodes, such as $LiCoO_2$[19], $Li_4Ti_5O_{12}$[20,21], and $LiFePO_4$[22]. The coating layers are usually deposited by radio frequency (RF) magnetron sputtering and atomic layer deposition method. Few literatures are available about the modification of $LiNi_{1/3}Co_{1/3}Mn_{1/3}O_2$ (NCM) electrodes.

In this research, the graphene oxide (GO) thin film was uniformly deposited on the traditionally prepared NCM electrodes by a simple screen-printing method. The results of galvanostatic charge-discharge test, cyclic voltammetry test, and electrochemical impedance spectra indicated that the rate capability and cycle stability were enhanced.

1 Experiment

The NCM powder (Shenzhen, N8-L), acetylene black (average grain size of 40 nm), polyvinylidene fluoride (PVDF, AR), and the aqueous solution of GO (Suzhou, Tanfeng) were used as the primary materials. Firstly, the uniform paste of NCM powder, acetylene black, graphite KS-6, and PVDF

Received date: September 11, 2020
Foundation item: National Natural Science Foundation of China (51705306); Shanghai Municipal Science and Technology Commission Project (15110501100); Open Fund of Jiangsu Laboratory of Lake Environment Remote Sensing Technologies of Huaiyin Institute of Technology (JSLERS-2019-003)
Corresponding author: Wang Ying, Ph. D., School of Mechanical and Automotive Engineering, Shanghai University of Engineering Science, Shanghai 201620, P. R. China, Tel: 0086-21-67791147, E-mail: wangyingcae@sues.edu.cn

were spread on the aluminum foil and air-dried in oven for 6~8 h, as mentioned in Ref.[23], with the mass ratio of 8:0.6:0.4:1. For the screen-printing process, the nylon screen mesh with wire of 20 μm in diameter and 20 μm in aperture was selected. The dry NCM electrode was placed on the vacuum metal surface of the automatic coating machine. Then, the mesh was placed on the electrode; 6 mL GO solution was extracted with the concentration of 2 $mg \cdot mL^{-1}$ using the pipette, and dropped evenly on the nylon wire. The electrode was scraped back and forth twice with the scraper. Finally, the coated electrodes were dried at 120 °C for 10 h. The fully dried electrodes were cut into small round pieces with 14 mm in diameter for battery assembling afterwards. The average area density of GO was 0.032 $mg \cdot cm^{-2}$.

For battery testing, two-electrode coin cells (CR2032) were assembled in an argon-filled glovebox with water index less than 0.735 $mg \cdot m^{-3}$. The primary and modified electrodes were used as cathodes with lithium foil as anodes, namely NCM and GO@NCM electrodes. Then 1 $mol \cdot L^{-1}$ $LiPF_6$ in ethylene carbonate (EC) and diethyl carbonate (DEC) solution (volume ratio of 1:1) was adopted as the electrolyte. The structure and morphology of primary and modified electrodes were characterized by X-ray diffraction (XRD, Bruker, D2-Phaser, Cu Kα) and scanning electron microscope (SEM, Hitachi, S-4800). Micro-Raman spectroscopy was performed on the primary and modified electrodes using a micro-Raman spectrometer from Renishaw inVia equipped with a laser of 532 nm, four charge-coupled-device (CCD) cameras, and an optical microscope (OM, Leica). The 50× objective lens was used to focus the incident beam and grating. The galvanostatic charge-discharge tests were condu-cted on CT2001A (Wuhan LAND electronics Co., Ltd). The reference voltage in this research was Li/Li^+. The potential was set within a range of 2.5~4.3 V. Cyclic voltammetry (CV, 2.5~4.3 V, 0.1 and 0.5 $mV \cdot s^{-1}$) and electrochemical impedance spectra (EIS, 3.6 V, 0.1~10 MHz, 10 mV) information were collected by an electrochemical workstation (CHI660E).

2 Results and Discussion

XRD patterns of the primary and GO modified NCM electrodes are shown in Fig. 1. The XRD patterns of modified electrodes have similar characteristics with those of primary electrodes. The 2θ at 18.0°, 36.0°, 37.6°, 43.7°, 48.0°, 58.0°, 63.7°, 64.3°, and 67.6° is referred as the plane of (003), (101), (006), (104), (105), (107), (108), (110), and (113), respectively. These peaks are indexed as the space group R-3m. The peak at 2θ=25.9° is caused by the (002) planes of graphite KS-6, which is a component of electrical additives. The XRD patterns of GO cannot be detected because the amount of GO in the modified electrodes is very small.

The formation of GO on the electrodes is confirmed by Raman spectroscopy. As shown in Fig. 2, from the Raman spectrum of GO modified NCM electrodes, the peaks observed at 479 and 589 cm^{-1} are attributed to the E_g and A_{1g} bands of NCM, respectively, indicating that the NCM have the R-3m symmetry. The relation between the peak index in the

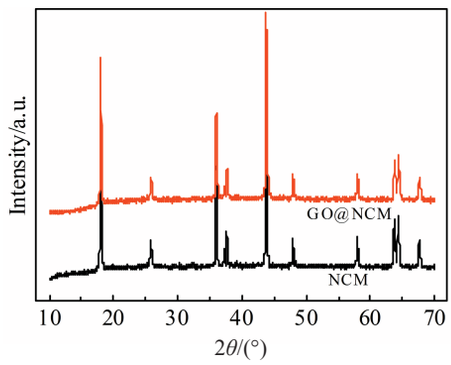

Fig.1 XRD patterns of primary and GO modified NCM electrodes

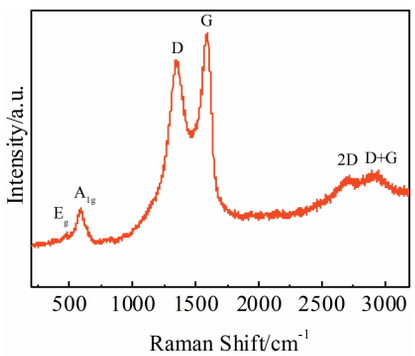

Fig.2 Raman spectrum of GO modified NCM electrode

XRD patterns and the R-3m symmetry of NCM is proved by the Raman spectrum[24]. The first-order scattering under E_{2g} mode in graphene and that under breathing mode in aromatic rings (very intense and broad) suggest that the typical broad bands at 1348 and 1596 cm^{-1} are D and G bands[25,26], respectively. Furthermore, the weak overtone regions of signals are also distinguished at 2696 and 2945 cm^{-1} [25-27]. The result confirms that the NCM are well coated by GO and the GO coating layer shows no detectable impact on the physical characteristics of NCM electrodes.

The SEM image of primary electrode is shown in Fig. 3a. The secondary particles with diameter of 0.1~20 μm are NCM. The flocculent material is carbon black, namely acetylene black. The flakes among the NCM particles and carbon black are graphite KS-6, which agrees with the XRD patterns (Fig. 1). For the GO modified specimens, the NCM secondary particles, carbon black, and graphite KS-6 flakes are all well covered by a thin GO layer, as shown in Fig.3b.

The corresponding batteries are charged and discharged at the rate of 31 $mA \cdot g^{-1}$ for 5 cycles. The reversible specific capacities of primary and GO modified NCM batteries are 161 and 163 $mAh \cdot g^{-1}$, respectively. The capacities of two batteries change to 145 and 144 $mAh \cdot g^{-1}$ when the charge-discharge current changes to 154 $mA \cdot g^{-1}$, as shown in Fig. 4. The capacity of all specimens decreases during the cycle test, whereas the decrease rate of GO modified electrodes is much slower than that of the primary electrodes. At 105th cycle, the capacity

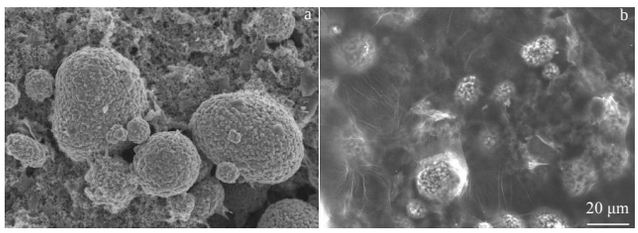

Fig.3 SEM images of primary (a) and GO modified (b) NCM electrodes

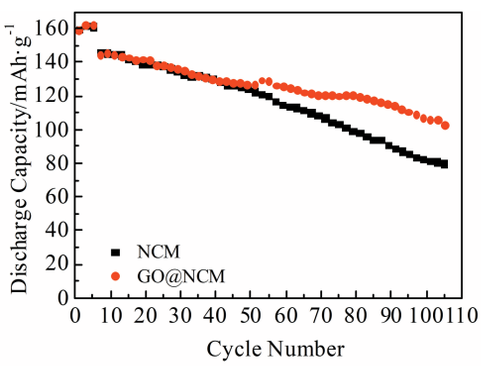

Fig.4 Cycle performance of primary and GO modified NCM electrodes

of the GO modified electrodes retains a high value of 103 mAh·g^{-1}, while the lower capacity of 80 mAh·g^{-1} is obtained for the primary electrodes.

To further illustrate the enhanced cycle performance, the typical charge-discharge curves and the corresponding dQ/dV profiles of 6th and 80th cycle of the primary and GO modified electrodes are shown in Fig. 5. Obviously, the voltage reduction of primary NCM electrodes during cycling is obviously restrained by GO modification, as shown in Fig. 5a. The polarization of the primary and GO modified NCM electrodes at 6th cycle is 0.0335 and 0.1296 V, increasing to 0.2049 and 0.3445 V at 80th cycle, respectively. The polarization of the primary electrodes is raised due to a large magnitude by more than 6 times after the charge-discharge tests, which is caused by the rapid degradation of the primary electrodes. For the GO modified electrodes, the polarization at 80th cycle is 2.6 times higher than that at 6th cycle, indicating a smaller polarization increment. Therefore, the polarization increment speed is effectively suppressed by the GO layer fabricated by screen-printing method. The suppressed voltage reduction and the lower polarization increment speed suggest a higher structure stability and enhanced cycle performance.

The discharge capacity of primary electrodes was tested at the current density of 31, 77, 154, 308, and 462 mA·g^{-1}, whose value is 161, 150, 132, 97, and 37 mAh·g^{-1}, respectively, as shown in Fig. 6a. For the GO modified electrodes, the discharge capacities improve to 163, 152, 134, 109, and 72 mAh·g^{-1} at different current densities. The capacity difference becomes larger with increasing the current density. The cyclic voltammetry tests were carried out at scan rates of 0.1 and 0.5 mV·s^{-1}. As shown in Fig. 6b, the obtained CV curves explain the reason for the improved rate capability. The potential shifting of oxidation and reduction peak of primary NCM electrodes is 0.166 V at the scan rate of 0.1 mV·s^{-1}, which is raised to 0.459 V when the scan rate is 0.5 mV·s^{-1}. The potential difference increases by ~1.8 times. However, the potential of GO modified electrodes only increases by 1.1 times. The potential shift values of the GO modified electrodes are 0.245 and 0.522 V at 0.1 and 0.5 mV·s^{-1}, respectively. For both primary and GO modified NCM electrodes, the peaks current increases with the increase of scanning rate. In addition, the oxidation and reduction peaks shift to higher and lower potential positions, respectively, suggesting the diffusion controlled behavior[28]. For diffusion controlled process, the Li^+ diffusion coefficient is computed by Randles-Sevcik formula[29,30] as follows:

$$I_p = 2.68 \times 10^5 n^{3/2} A D^{1/2} C v^{1/2} \quad (1)$$

where I_p is the peak current intensity, n is the number of electrons per reaction species (n=1), A is the surface area of the electrode, D represents the diffusion coefficient, C is the molar concentration of Li in NCM (~4.943×10^{-2} mol·cm^{-3}), and v is the scan rate. According to Eq. (1), the plot of the reduction peak current intensity I_p versus the square root of the scan rate ($v^{1/2}$) should be a straight line, and the slope can be estimated as the diffusion coefficient, as shown in Fig.7.

Obviously, the slope of relationship line of GO@NCM electrodes is larger, indicating that the diffusion process is faster. Besides, for GO@NCM and NCM electrodes, the Li^+

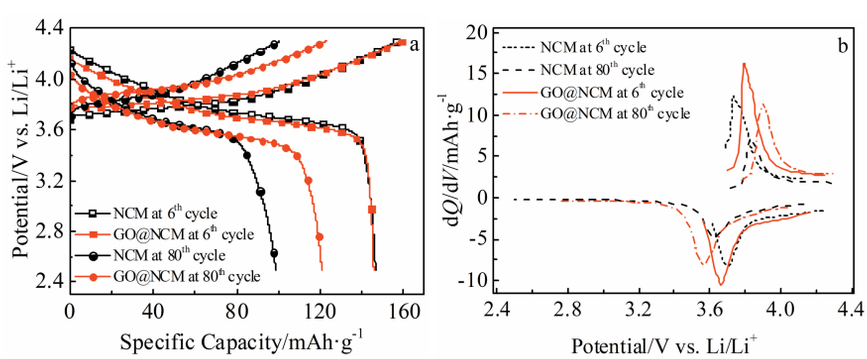

Fig.5 Charge-discharge curves (a) and corresponding dQ/dV profiles (b) of primary and GO modified NCM electrodes at 6th and 80th cycles

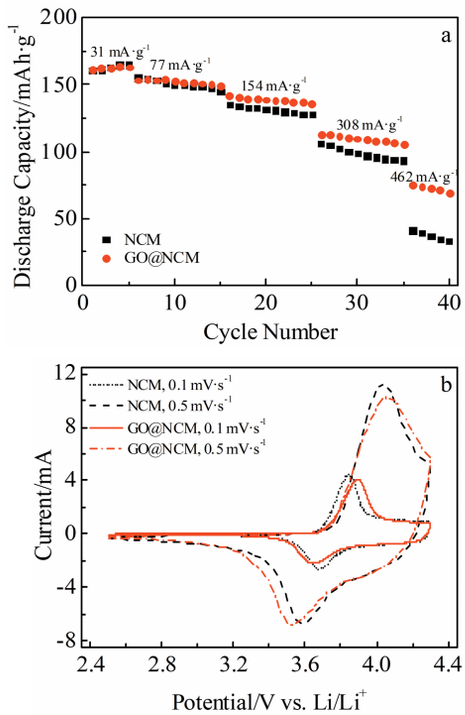

Fig.6 Discharge capacity (a) and cyclic voltammetry profiles at different scan rates (b) of primary and GO modified NCM electrodes

diffusion coefficient (D_{Li^+}) is 3.69×10^{-10} and 2.82×10^{-10} $cm^2\cdot s^{-1}$, respectively. The GO@NCM electrodes have higher diffusion coefficient than the NCM electrodes do. Based on the above results, it can be concluded that the GO modified NCM electrodes have a faster transfer process for lithium ions and a better reversibility of the electrode reaction.

The electrochemical impedance plots of primary and GO

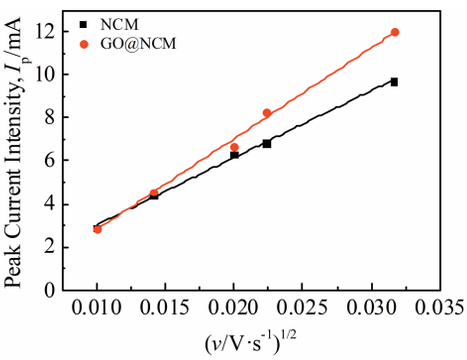

Fig.7 Relation between peak current intensity I_p and scan rate for primary and GO modified NCM electrodes

modified NCM electrodes are shown in Fig. 8. As shown in Fig. 8a, the high frequency semicircle is ascribed to the charge transfer behavior in the interface of the electrode and electrolyte (R_{ct}). The R_{ct} of GO modified electrodes is greater than that of primary electrodes by 200 Ω for newly assembled batteries, as shown in Table 1. After screen-printing, the GO thin film with high resistance towards the aggressive environment forms on the electrode surface during the secondary drying process[31,32]. The thin film reduces the direct contact between the NCM electrodes and the electrolyte. The coating layer of GO suppresses the side reaction between NCM electrodes and electrolyte, showing a marked increase in the charge transfer resistance. There is no obvious semicircle arising from SEI film for the newly assembled batteries. The most likely reason is that SEI film barely forms during the test. The Nyquist plots of the cycled batteries consist of more than one semicircle, as shown in Fig. 8b. There is one new semicircle for cycled primary electrodes, which is ascribed to the SEI film formation after CV tests. Meanwhile, two

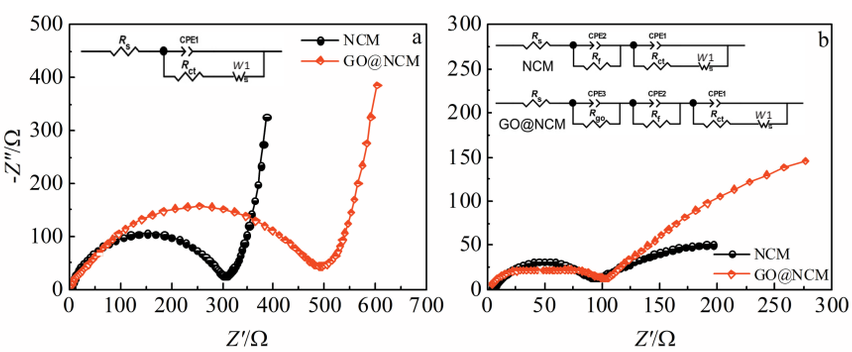

Fig.8 EIS plots of primary and GO modified electrodes of freshly assembled (a) and cycled (b) batteries

new semicircles appear for the cycled GO modified electrodes, referring to the resistances of GO (R_{GO}) and SEI film.

The fitted R_{ct} of the GO modified electrodes is 229 Ω, as shown in Table 1, which is larger than that of the primary electrodes. The increasing R_{ct} suggests a larger polarization, which agrees with the charge-discharge test results. The reduction of SEI film resistance (R_f) of GO modified

Table 1 Fitted data of primary and GO modified electrodes (Ω)

Battery state	Electrode	R_{GO}	R_f	R_{ct}
Freshly assembled	NCM	-	-	272
	GO@NCM	-	-	472
Cycled	NCM	-	91	105
	GO@NCM	36	65	229

electrodes indicates the better cycle performance and rate capability.

3 Conclusions

1) The uniform graphene oxide (GO) coating was fabricated by the screen-printing method on $LiNi_{1/3}Co_{1/3}Mn_{1/3}O_2$ (NCM) electrodes.

2) The GO coating layer shows no detectable impact on the physical characteristics of NCM electrodes. GO modified NCM electrodes exhibit elevated rate capability and cycle performance. The performance improvement is ascribed to the faster transfer of lithium ions.

3) The GO coating layer suppresses the degradation of the NCM electrodes by restraining the polarization increment during the galvanostatic charge-discharge tests and restricts the potential shifting between the redox peaks at high scan rate.

References

1 Liang C, Kong F, Longo R C *et al. The Journal of Physical Chemistry C*[J], 2016, 120(12): 6383
2 Choi J W, Aurbach D. *Nature Reviews Materials*[J], 2016, 1(4): 16 013
3 Liu W, Oh P, Liu X *et al. Angewandte Chemie International Edition*[J], 2015, 54(15): 4440
4 Hu M, Pang X L, Zhou Z. *Journal of Power Sources*[J], 2013, 237: 229
5 He P, Yu H J, Li D. *Journal of Materials Chemistry*[J], 2012, 22(9): 3680
6 Wu Y, Cao C B, Zhu Y Q *et al. Journal of Materials Chemistry A*[J], 2015, 3(30): 15 523
7 Han Z H, Yu J P, Zhan H *et al. Journal of Power Sources*[J], 2014, 254: 106
8 Kim H, Kim M G, Jeong H Y *et al. Nano Letters*[J], 2015, 15(3): 2111
9 Ren Y, Wang Y, Zhang W L *et al. RSC Advances*[J], 2019, 9(51): 29 760
10 Du Fuming, Zhao Ning, Fang Rui *et al. Journal of Inorganic Materials*[J], 2018, 33(4): 462
11 Zheng H H, Sun Q N, Liu G *et al. Journal of Power Sources*[J], 2012, 207: 134
12 Jung S K, Gwon H, Hong J *et al. Advanced Energy Materials*[J], 2014, 4(1): 1 300 787
13 Kondrakov A O, Schmidt A, Xu J *et al. The Journal of Physical Chemistry C*[J], 2017, 121(6): 3286
14 Evertz M, Horsthemke F, Kasnatscheew J *et al. Journal of Power Sources*[J], 2016, 329: 364
15 Stiaszny B, Ziegler J C, Krauß E E *et al. Journal of Power Sources*[J], 2014, 251: 439
16 Cho W, Kim S M, Song J H *et al. Journal of Power Sources*[J], 2015, 282: 45
17 Cho W, Kim S M, Lee K W *et al. Electrochimica Acta*[J], 2016, 198: 77
18 Zhou A J, Wang W H, Liu Q *et al. Journal of Power Sources*[J], 2017, 362: 131
19 Zhou A J, Lu Y T, Wang Q J *et al. Journal of Power Sources*[J], 2017, 346: 24
20 Wang Y, Zou W, Huang Z *et al. ECS Transactions*[J], 2014, 59(1): 35
21 Wang Y, Ren Y, Dai X Y *et al. Royal Society Open Science*[J], 2018, 5(10): 180 762
22 Tan G, Wu F, Li L *et al. The Journal of Physical Chemistry C*[J], 2013, 117(12): 6013
23 Wang Y, Zhou A J, Dai X Y *et al. Journal of Power Sources*[J], 2014, 266: 114
24 He J R, Chen Y F, Li P J *et al. RSC Advances*[J], 2014, 4(5): 2568
25 Wang R B, Li W W, Liu L T *et al. Journal of Electroanalytical Chemistry*[J], 2019, 833: 63
26 Zhang J, Zhou R, Minamimoto H *et al. Applied Materials Today*[J], 2019, 15: 372
27 Pérez L A, Bajales N, Lacconi G I. *Applied Surface Science*[J], 2019, 495: 143 539
28 Chen Z, Wang J, Chao D L *et al. Scientific Reports*[J], 2016, 6: 25 771
29 Vasu S, Sahana M B, Sudakar C *et al. Electrocimica Acta*[J], 2017, 251: 363
30 Hou L N, Qin X, Gao X J *et al. Journal of Alloys and Compounds*[J], 2019, 774: 38
31 Chauhan D S, Quraishi M A, Ansari K R *et al. Progress in Organic Coatings*[J], 2020, 147: 105 741
32 Kumar M K P, Laxmeesha P M, Ray S *et al. Applied Surface Science*[J], 2020, 533: 147 512

丝网印刷氧化石墨烯对锂离子电池 $LiNi_{1/3}Co_{1/3}Mn_{1/3}O_2$ 三元正极的改性及性能影响

张文龙[1]，王　影[1,2]，王东征[1]，鲁春驰[1]，严　晓[1]，黄碧雄[1]

(1. 上海工程技术大学 机械与汽车工程学院，上海 201620)

(2. 淮阴工学院 江苏省湖泊环境遥感技术工程实验室，江苏 淮安 223003)

摘　要：通过丝网印刷方法，在由$LiNi_{1/3}Co_{1/3}Mn_{1/3}O_2$、导电添加剂和聚偏氟乙烯制成的电极表面涂覆了一层薄薄的氧化石墨烯。在充电截止电压为4.3 V的条件下进行了循环性能和倍率性能测试。结果表明：未改性电极在恒电流充放电测试中容量下降且极化增加，而包覆改性后电极的容量衰减程度和极化增加速度降低。这是由于氧化石墨烯涂层抑制了$LiNi_{1/3}Co_{1/3}Mn_{1/3}O_2$电极和电解质之间的部分副反应，使得改性电极的循环稳定性和倍率性能显著提高，为提升$LiNi_{1/3}Co_{1/3}Mn_{1/3}O_2$电极性能提供了一种环境友好且非常有效的方法。

关键词：$LiNi_{1/3}Co_{1/3}Mn_{1/3}O_2$；正极；氧化石墨烯；丝网印刷；锂离子电池

作者简介：张文龙，男，1996年生，硕士，上海工程技术大学机械与汽车工程学院，上海 201620，E-mail：sues_zhangwenlong@163.com